

# Optimal description of forced zonal mean tropical precipitation changes.

A. Donohoe<sup>1</sup>, A.R. Atwood<sup>2</sup>, D.S. Battisti<sup>3,4</sup>

<sup>1</sup>Polar Science Center, Applied Physics Laboratory, University of Washington, Seattle, Washington 98195, USA.

<sup>2</sup>Florida State University, Department of Earth Ocean and Atmospheric Science

<sup>3</sup>Department of Atmospheric Sciences, University of Washington, Seattle, Washington 98195, USA.

<sup>4</sup>

## Key Points:

- The simulated response of the zonal mean tropical precipitation ( $\Delta P$ ) to paleoclimate, anthropogenic and volcanic forcing is analyzed in terms of optimal shifts, contractions and intensifications of the climatological unperturbed precipitation .
- ITCZ shifts are small in magnitude and describe a small fraction  $\Delta P$  whereas intensification and contractions are tightly anti-correlated and describe a large portion of the  $\Delta P$ .
- The annual mean response is best characterized as a modification of the climatological seasonal cycle; annual shifts correspond to an intensification during on solstice and contractions to reduced seasonal migration of the ITCZ.

---

Corresponding author: A. Donohoe, [adonohoe@u.washington.edu](mailto:adonohoe@u.washington.edu)

**Abstract**

Place Holder.

**1 Introduction**

Meridional shifts in the region of intense tropical precipitation – the intertropical convergence zone (ITCZ) – are often invoked to explain paleoclimate proxy records of precipitation at single and/composites of sites in the tropics and subtropics. Here, we examine how useful the concept of a meridional shift of the climatological precipitation pattern is for explaining precipitation changes in response to external forcings (e.g. anthropogenic, paleoclimatic boundary conditions and freshwater hosing) in comprehensive climate model simulations. We also explore how the shift in the location of simulated tropical precipitation varies by longitude (i.e. between the different ocean basins). We demonstrate the meridional ITCZ shift– defined as the north-south translation of the unperturbed annual mean precipitation – explains a very small portion of the local ( $< 1\%$ ) and zonal mean ( $< 9\%$ ) precipitation changes in the ensemble average response to a myriad of external forcings. We further consider two additional modes of ITCZ variability: the meridional contraction/expansion of the tropical precipitation and the amplification/reduction of the tropical precipitation with the same spatial structure as the climatology. The amplifying mode explains the greatest fraction of local (8%) and zonal mean (35%) precipitation changes over the ensemble of forcing experiments. The contracting mode explains a smaller fraction of tropical precipitation changes than the amplifying mode (3% locally and 20% in the zonal average) but is a more useful theoretical construct for thinking about large scale patterns of precipitation change than the idea of a meridional ITCZ shift. These results demonstrate that tropical precipitation changes seen in paleoclimate records and anticipated in the future are influenced by the following processes listed in order of decreasing importance: 1.) localized circulation changes leading to zonal inhomogeneities in precipitation anomalies, 2.) tropics wide (spatially invariant) amplification/reduction of the hydrological cycle, 3.) meridional contraction/expansion of the region of intense pre-

45 precipitation and 4.) the meridional shift of the climatological precipitation. We emphasize  
46 that ITCZ shift is the least influential mode of tropical precipitation changes and speculate  
47 that the often invoked ITCZ shift deduced invoked in paleoclimate studies reflect localized  
48 changes as opposed to large scale modes of climate variability.

## 49 **2 Model simulations analyzed and methodology**

50 We analyze tropical precipitation changes in coupled model simulations under pa-  
51 leoclimatic (e.g. glacial boundary conditions, freshwater hosing and mid-Holocene or-  
52 bital forcing) and anthropogenic (increased atmospheric CO<sub>2</sub>) forcings. We ask how much  
53 of these precipitation changes are explained by each: 1. meridional shifts (translation), 2.  
54 meridional contraction and 3. domain wide intensification of the climatological pattern on  
55 tropical precipitation. Here, we outline the model simulations and methodology used for  
56 answering this question.

### 57 **2.1 Model simulations**

58 We examine precipitation changes in 4 different sets of forcing experiments, each in  
59 an ensemble of coupled climate models. A total of 42 simulations are analyzed.

- 60 **1. Last Glacial Maximum (LGM).** We use model output from the Paleoclimate Mod-  
61 eling Intercomparison Project phase 2 (PMIP2) project, an ensemble of state of  
62 the art coupled (ocean-atmosphere-cryosphere) model simulations run under pre-  
63 scribed forcing and boundary condition scenarios that represent different paleocli-  
64 matic epochs. The Last Glacial Maximum (LGM) simulations are forced by solar  
65 insolation from 21,000 years before present, greenhouse gas and aerosol concen-  
66 trations deduced from ice core data (CO<sub>2</sub> is set to 185 ppm) which amounts to a  
67 radiative forcing of approximately  $-2.8 \text{ W m}^{-2}$  [Braconnot *et al.*, 2007], coastlines  
68 consistent with a 120m decrease in sea level, and the prescribed land ice topogra-  
69 phy of *Peltier* [2004] which includes the expansive Laurentide ice sheet over North

70 America. We use the LGM simulations with fixed vegetation (PMIP2 OA runs).  
71 All comparisons are made to the pre-industrial simulations in the same model and  
72 resolution. 12 simulations are analyzed.

73 **2. Mid-Holocene.** Mid Holocene runs are taken from the PMIP3 [*Braconnot et al.*,  
74 2012] simulations of the climate system approximately 6,000 years ago. Coastlines,  
75 vegetation, and ice sheets are identical to the PI simulations. CO<sub>2</sub> and aerosols are  
76 also identical to the PI while there is a modest reduction in methane concentration  
77 [*Taylor et al.*, 2012]– from 760 ppbv to 650 ppbv. Orbital parameters representative  
78 of 6,000 years before present are taken from *Berger* [1978]. Most significantly, or-  
79 bital precession causes the seasonal cycle of insolation in the Northern Hemisphere  
80 to amplify, while the duration of summer is reduced. We note that the sum of all  
81 mid-Holocene forcing agents are symmetric about the equator in the annual aver-  
82 age. Seven different model simulations are analyzed.

83 **3. Hosing experiments.** Placeholder for description. 7 models with Axel's.

84 **4. 4XCO<sub>2</sub>.** We analyze the CMIP5 instantaneous CO<sub>2</sub> quadrupling [*Taylor et al.*,  
85 2012]. Each model is initialized from the equilibrated pre-industrial (PI). Atmo-  
86 spheric carbon dioxide is instantaneously quadrupled and is then held fixed there-  
87 after. We calculate the climatology of each model over the last 20 years of simu-  
88 lations and then take differences relative to the climatology in the PI (or PD) run.  
89 Sixteen different models are analyzed.

## 90 **2.2 Methodology**

91 Paleoclimatic and modeled precipitation changes are commonly interpreted in terms  
92 of an ITCZ shift defined as a meridional translation of the climatological pattern of pre-  
93 cipitation in the tropics. Such shifts are often invoked to explain the zonal mean and two-  
94 dimensional (latitudinal-longitudinal) structure of precipitation changes – hereafter refer-  
95 red to as local. In both the local and zonal mean cases, a northward ITCZ shift results

96 in an increase in precipitation at tropical locations <sup>1</sup> North of the climatological precip-  
97 itation maximum and a concurrent decreases in precipitation at locations on or South of  
98 the tropical precipitation maximum. To test how well this theoretical construct of tropical  
99 precipitation variability works in explaining the precipitation changes, we take the clima-  
100 tological pattern of tropical precipitation – defined as equatorward of 20°– from the PI  
101 simulation in each model and shift it North and South (hereafter referred to as the shifted  
102 precipitation) until we achieve an optimal fit to the perturbed precipitation pattern under  
103 the forcing. We optimize the shift for both the local pattern of precipitation changes–  
104 whereby the latitudinal/longitudinal structure of precipitation is shifted North and South  
105 by the same amount at each longitude (upper left panel of Figure 1 shows a 5° northward  
106 shift) – and zonal mean precipitation change – whereby the PI zonal mean precipitation is  
107 simply shifted North and South to best match the perturbed zonal mean (upper right panel  
108 of Figure 1). To achieve the shifted precipitation, we interpolate the PI precipitation to  
109 a 0.5 degree grid with the shift added to the input latitude and compare to the perturbed  
110 precipitation interpolated to the same 0.5 degree grid. Grid resolution was found to have  
111 a minimal impact on the results. We define the optimal shift as that which minimizes the  
112 root mean squared difference between the shifted precipitation and the precipitation in the  
113 forced simulation spatially averaged over the tropics. We note that the optimal shift for the  
114 local and zonal mean cases need not be (and often are not) the same as the local shift will  
115 be optimized when precipitation increases North/South of regions (longitudes) of climato-  
116 logically intense precipitations where as the zonal mean optimization does not account for  
117 whether the longitudinal structure of the climatological and perturbed precipitation match  
118 each other.

---

<sup>1</sup> For the purposes of this study, we define the tropics as equatorward of 20<sup>l</sup>° although, for the discussion here, the region equatorward of the subtropical precipitation minimum would be expected to follow juxtaposing precipitation changes North and South of the tropical precipitation maximum

119           Additionally, we consider two more modes of ITCZ variability: a meridional contrac-  
120           tion and a domain wide intensification. The contraction mode is defined by multiplying  
121           the input latitude by a scalar prior to interpolating to the 0.5 degree grid. The scalar of  
122           1 would redefine the PI precipitation, scalars  $> 1$  correspond to expansion of the tropi-  
123           cal precipitation and scalars  $< 1$  correspond to contraction (middle panel of Figure 1).  
124           The intensification mode is defined by taking the spatial pattern of precipitation in the PI  
125           simulation and simply multiplying it by a scalar; it represents an intensification of the pre-  
126           cipitation with no changes in the underlying spatial structure (lower panel of Figure 1).

127           All three modes of variability are considered simultaneously to optimize the fit to  
128           the perturbed tropical precipitation; starting from the PI precipitation, the pattern of com-  
129           bined shifted, contracted and intensified precipitation that minimizes the RMS difference  
130           with the GCM precipitation from the perturbed simulation is considered the best answer.  
131           To achieve this answer, we start by optimizing the fit to the perturbed precipitation for  
132           each mode (shift/contraction/intensification) separately, starting from the PI precipitation  
133           as a first iteration. We then repeat the optimization of each mode starting from the opti-  
134           mal answers provided by the other modes in the previous iteration. For example, in itera-  
135           tion number 2, we optimize the shifting mode by starting from the contracted and inten-  
136           sified PI precipitation defined by the optimal contraction and intensification in iteration 1  
137           and then finding the shift in that starting precipitation pattern that minimizes the RMS dif-  
138           ference from the perturbed precipitation spatially averaged over the tropics. This process is  
139           equivalent to considering all possible modes of variability simultaneously but is computa-  
140           tionally less demanding. 10 iterations are sufficient to converge on the optimal answer.

141           The optimal mode of shifting/contraction/intensification found by the above consider-  
142           ation of combined modes of variability agrees reasonable well with the optimal shift/contraction/intensification  
143           that is found when considering a mode of variability in isolation (e.g. optimizing from the  
144           PI precipitation). However, in some cases it differs substantially, including a reversal of  
145           directionality and does so in fairly systematic ways for a given forcing experiment. For

146 example, the global warming in the 4XCO<sub>2</sub> simulations results in increased tropical precipi-  
 147 tation which intuitively should be captured by the intensification mode. However, an  
 148 expansion of the tropical precipitation also results in a domain average increase in precipi-  
 149 tation since the precipitation closer to the equator exceeds that on the edge of our tropi-  
 150 cal domain (20°) in all PI models. Therefore, when considered in isolation, the contrac-  
 151 tion mode can capture the domain average precipitation increase even the spatial structure  
 152 of the precipitation is unchanged and, thus, can confuse an a scalar intensification with a  
 153 genuine contraction of the precipitation; the shifting, contraction and intensification modes  
 154 of precipitation changes are not orthogonal over the tropical domain. In the specific ex-  
 155 ample above, when the contraction mode is considered in isolation, the ensemble average  
 156 contraction to optimize the fit to precipitation under 4XCO<sub>2</sub> is not significantly different  
 157 from unity (0.99 ± 0.03 – 1 σ) where as a robust contraction (0.91 ± 0.03) is found when  
 158 all modes are allowed to operate simultaneously.

159 The fraction of precipitation change explained by the best answer,  $F_{S,C,I}$  (where the  
 160 subscripts denote Shifted, Contracted and Intensified) is given by

$$F_{S,C,I} = 1 - \frac{\sqrt{(P_{perturbed} - P_{S,C,I})^2}}{\sqrt{(P_{pert})^2}} \quad (1)$$

161 where  $P_{S,C,I}$  is the optimally shifted, contracted and intensified PI precipitation,  $P_{pert}$   
 162 is the simulated precipitation under forcing in the same model and  $\overline{\quad}$  denote the  
 163 spatial average over the tropical domain. We define the fraction of precipitation change ex-  
 164 plained by a single mode as the reduction in the fraction of precipitation explained when  
 165 that mode of variability is eliminated from the best answer. For example, the fraction of  
 166 precipitation change explained by the shifting mode is

$$F = F_{S,C,I} - F_{C,I} = \frac{\sqrt{(P_{perturbed} - P_{C,I})^2} - \sqrt{(P_{perturbed} - P_{S,C,I})^2}}{\sqrt{(P_{pert})^2}} \quad (2)$$

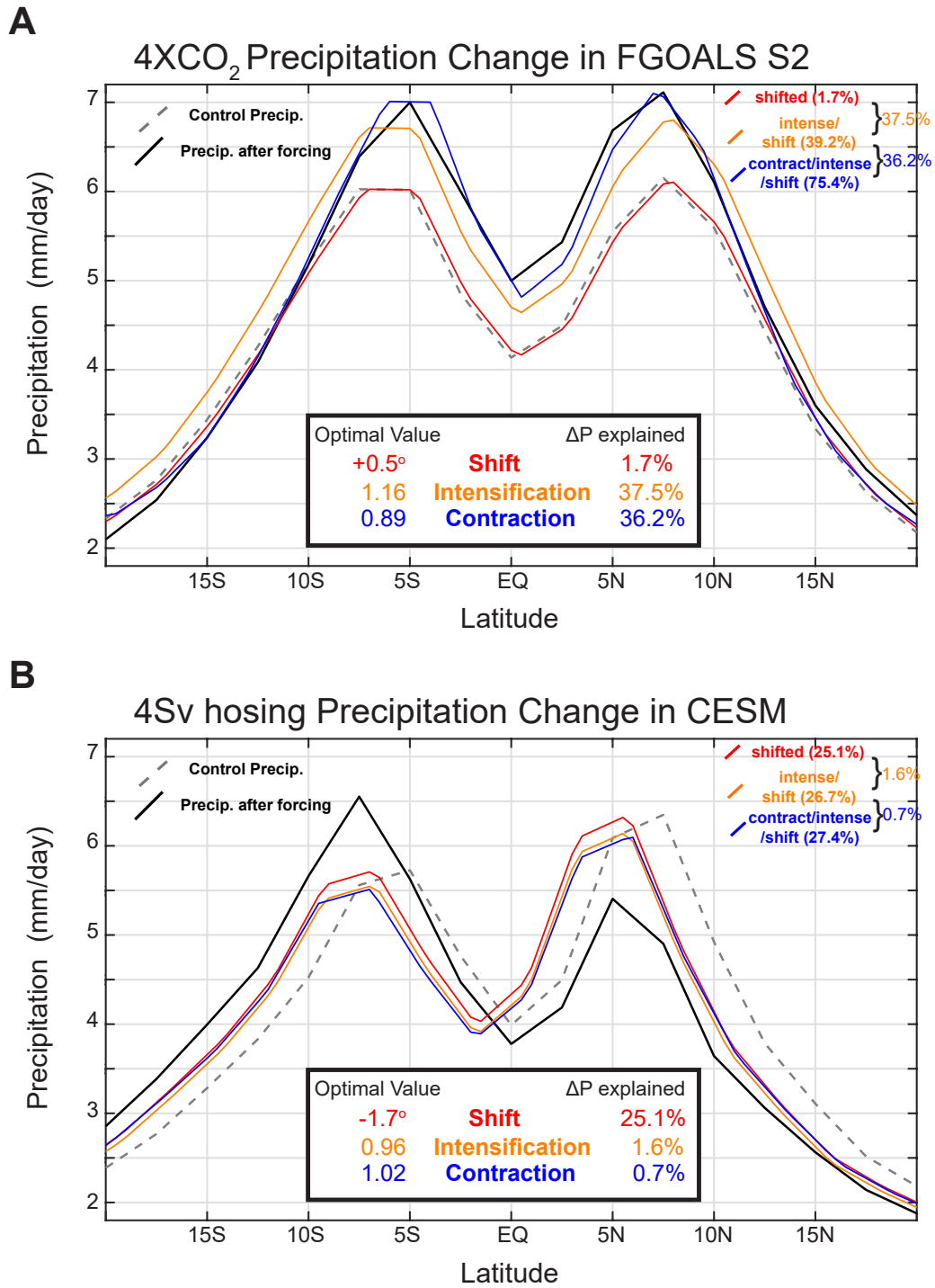
167 where the  $P_{C,I}$  is the contracted and intensified precipitation without the shift and the  
168 shift/intensification are taken from the optimization in the best (combined) answer. Qual-  
169 itatively similar results are found if the fraction of explained precipitation is defined as  
170 the fraction of precipitation explained if the PI is shifted by the best answer shift or if the  
171 PI precipitation is optimally shifted although both cases lead to the sum of the fractional  
172 precipitation changes explained by all three modes exceeding the  $F_{S,C,I}$  due to the non-  
173 orthogonality of the modes.

### 184 **3 Results**

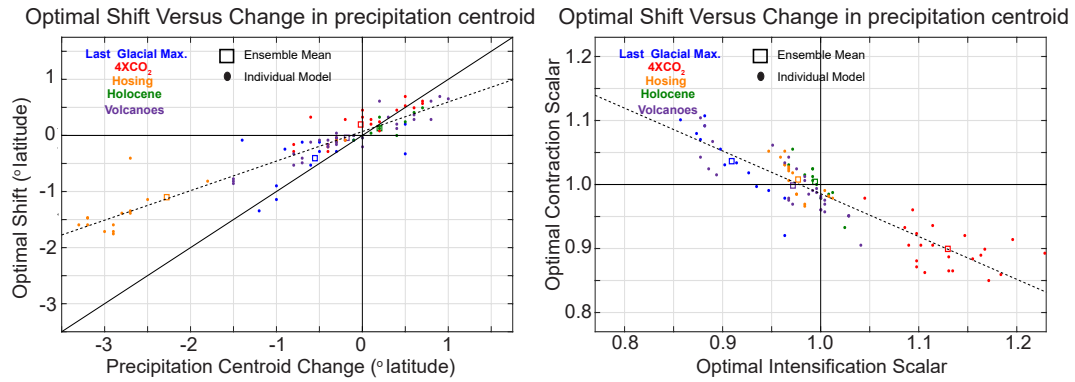
185 We discuss the tropical precipitation shifts, contractions and intensifications that  
186 best match the ensemble of perturbed forcing experiments and how well those modes of  
187 precipitation variability describe the tropical precipitation changes. The overarching con-  
188 clusion of this analysis is that the shifting mode explains a very small percentage of the  
189 precipitation changes, the contraction and intensification modes are more useful modes for  
190 thinking about precipitation changes but still fail to capture much of the tropical precipita-  
191 tion changes in the zonal mean but especially in the local structure.

#### 230 **3.1 Shifting mode**

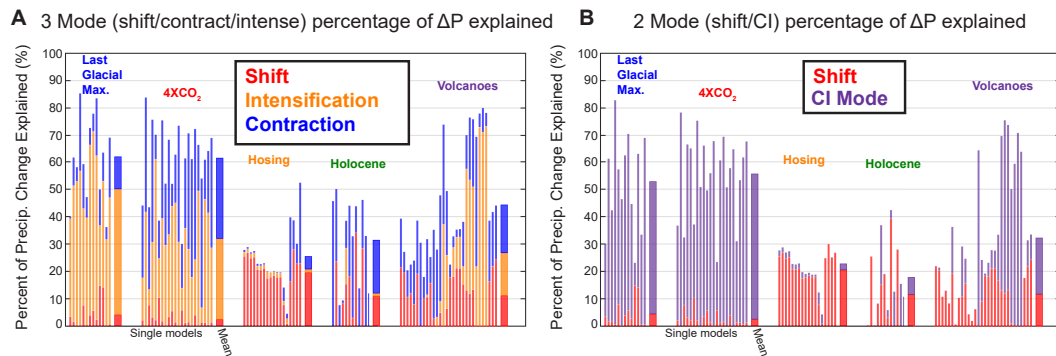
231 The meridional shift that optimizes the fit to the perturbed precipitation is small in  
232 magnitude ( $< 1^\circ$ ) and differs drastically between models even within the same experi-  
233 ment type; the optimal shift – for both the zonal mean and 2D structure– is not signif-  
234 icantly different from zero in the LGM and 4XCO<sub>2</sub> experiments, shows a small ( $0.2^\circ$ )  
235 northward shift of marginal (90% confidence interval ) significance in the mid-Holocene  
236 and is robustly southward (average of  $1^\circ$ ) in the heavily forced hosing experiments (Table  
237 1). Overall, the optimal zonal mean precipitation shift is well correlated with other met-  
238 rics of ITCZ shifts that have been used in the literature such as the centroid of the zonal  
239 mean precipitation equator-ward of  $20^\circ$  [Frierson and Hwang, 2012; Donohoe et al., 2013]  
240 with a correlation coefficient of 0.9 (Figure ??A). However, the magnitude of the optimal



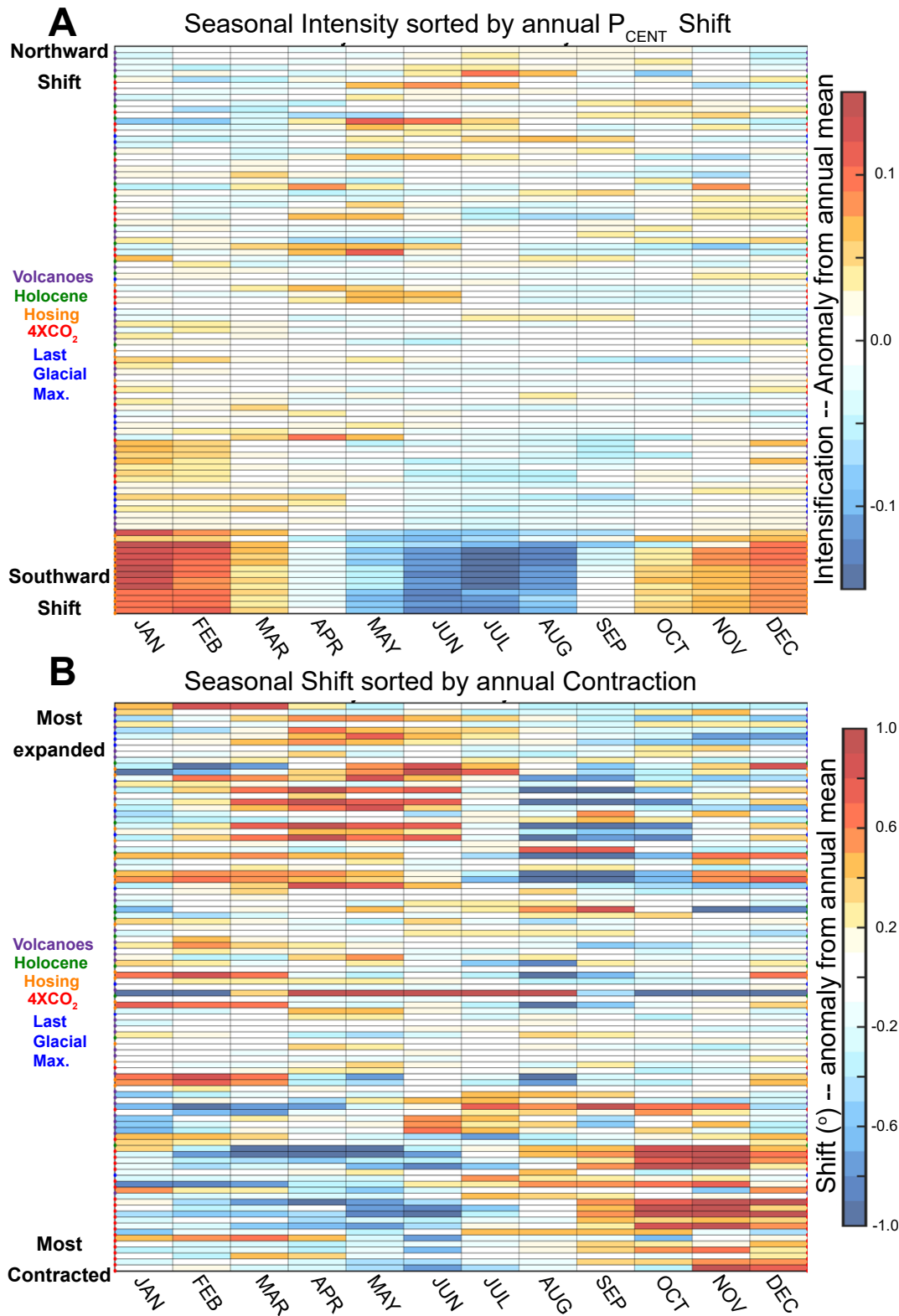
174 **Figure 1.** Illustration of optimal fitting to shifted/contracted/intensified modes of tropical precipitation and  
 175 the procedure used to define the percent of the precipitation change explained by each mode. The dashed gray  
 176 line shows the climatological (zonal and annual mean) precipitation in the control (preindustrial) simulations  
 177 and the black line shows the precipitation after external forcing. First the precipitation is optimally shifted (red  
 178 line). Next the precipitation is optimally intensified and shifted together (orange line). Finally, the precipita-  
 179 tion is optimally contracted, intensified and shifted together (blue). The percentage of  $\Delta P$  explained by each  
 180 mode is defined as the additional reduction in RMS  $\Delta P$  by successively introducing the mode and all optimal



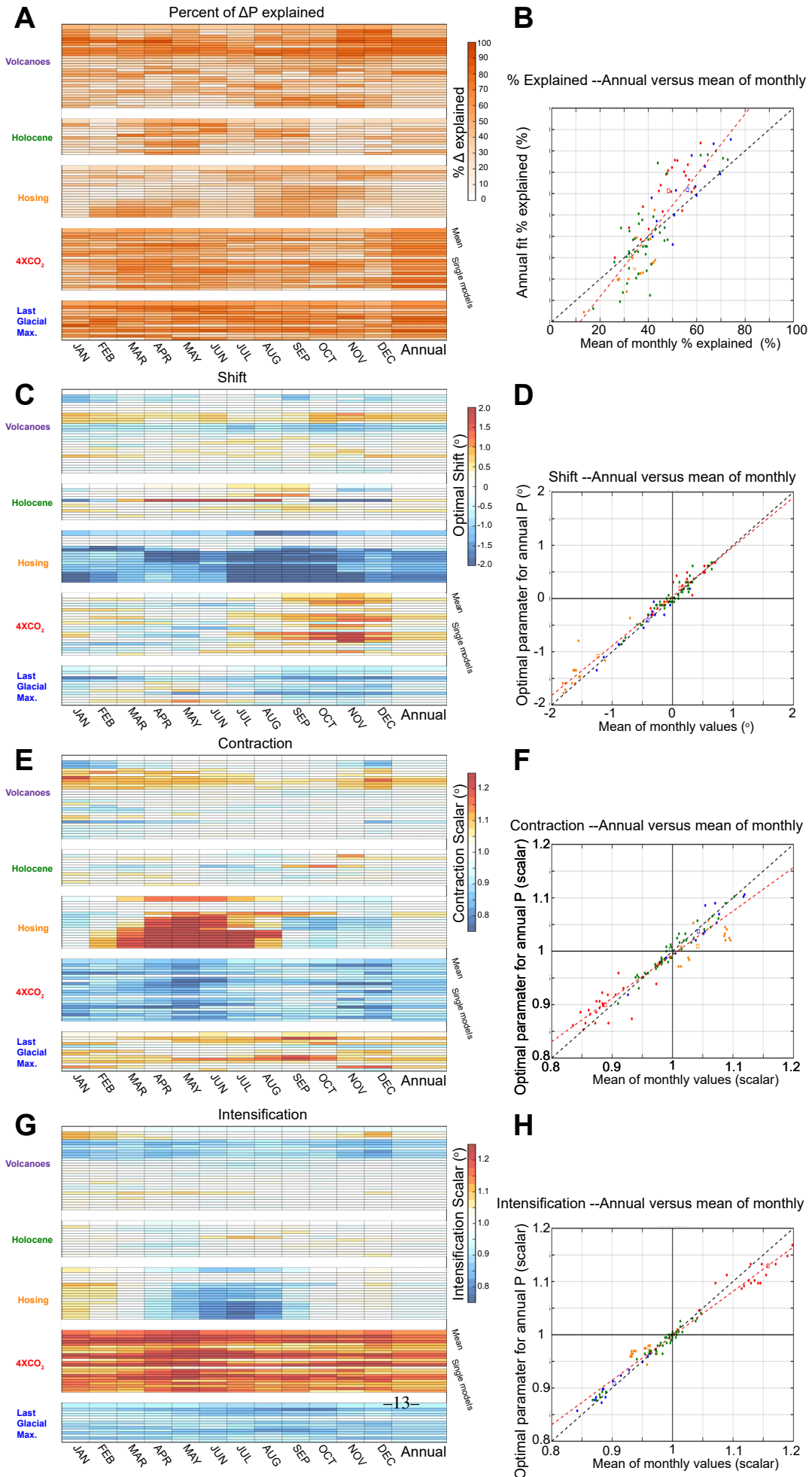
192 **Figure 2.** Optimal shift, contraction and intensification parameters for the zonal and annual mean precipi-  
 193 tation changes in response to LGM (blue), 4XCO<sub>2</sub> (red), Mid-Holocene (green), freshwater hosing (orange)  
 194 and volcanic (purple) forcing. (A) Optimal shift (abscissa) versus the change in precipitation centroid (ordi-  
 195 nate) that is commonly used to quantify ITCZ shifts. (B) Contraction scalar (abscissa) versus intensification  
 196 scalar (ordinate). The 1:1 line is shown by the solid black line and the linear best fit is shown by the dashed  
 197 black line. Dots represent individual models and the square shows the ensemble mean of simulations for each  
 198 forcing experiment.

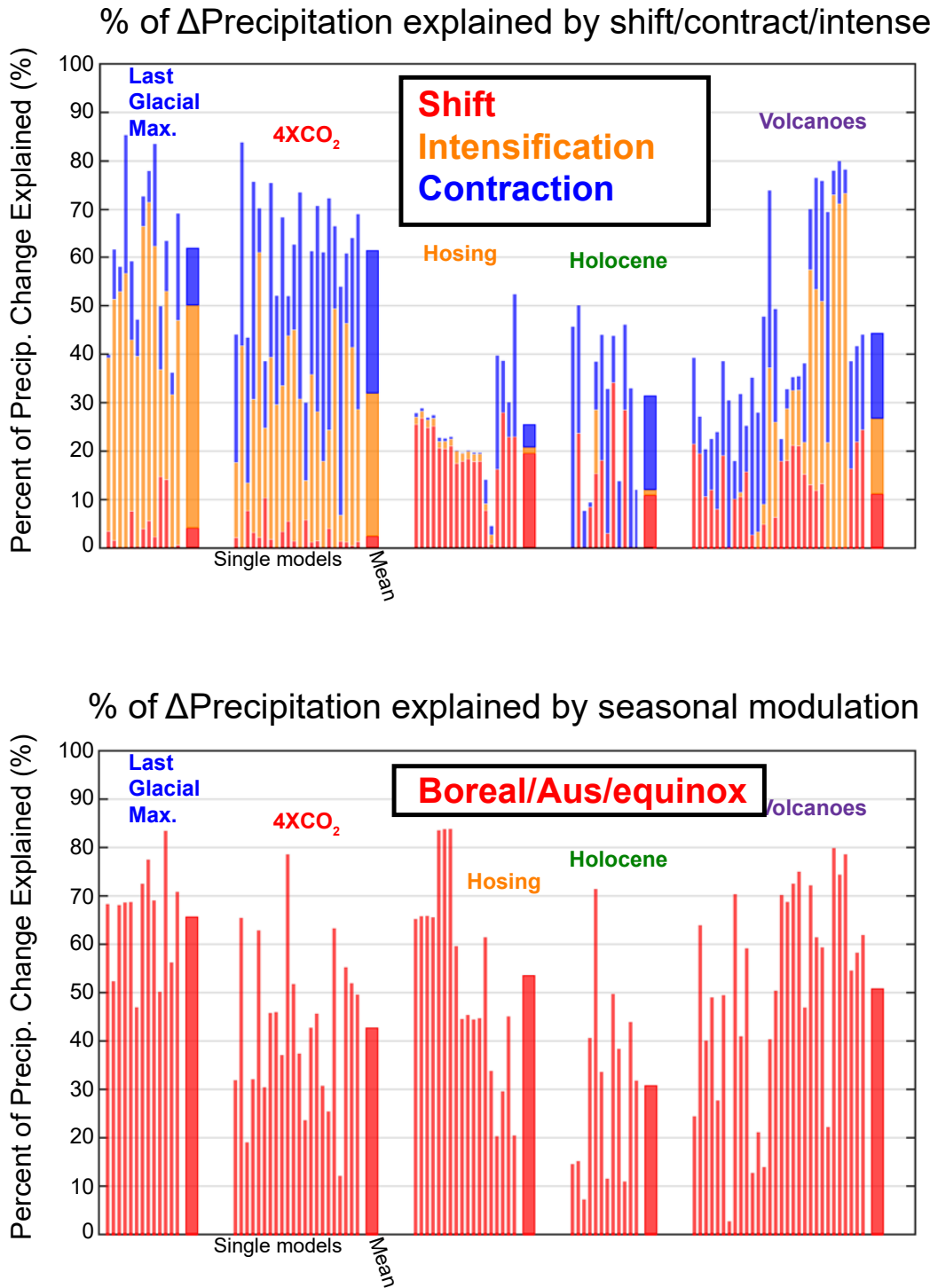


199 **Figure 3.** The percentage of  $\Delta P$  explained by each mode of tropical precipitation changes in the ensemble  
 200 of forced simulations. Results are grouped by forcing type with individual models shown by thin bars and the  
 201 ensemble average shown in the thick bar to the right. (A) Three mode optimization with percentages defined  
 202 starting from the shifting mode only (red) then adding the intensification mode (orange) and the adding the  
 203 contraction (blue). (B) Two mode optimization with percentages defined starting from the shifting mode (red)  
 204 then adding the combined contraction-intensification mode (CI – purple) with the ratio of the contraction to  
 205 intensification defined from the linear best fit across all simulations shown in Fig. 1B. The loss of percent-  
 206 age explained going from 3 to 2 modes is: total (7.4) LGM(8.7) 4XCO<sub>2</sub> (5.4) Hosing(2.0) Holocene(8.3)  
 207 Volcanic(11.2)



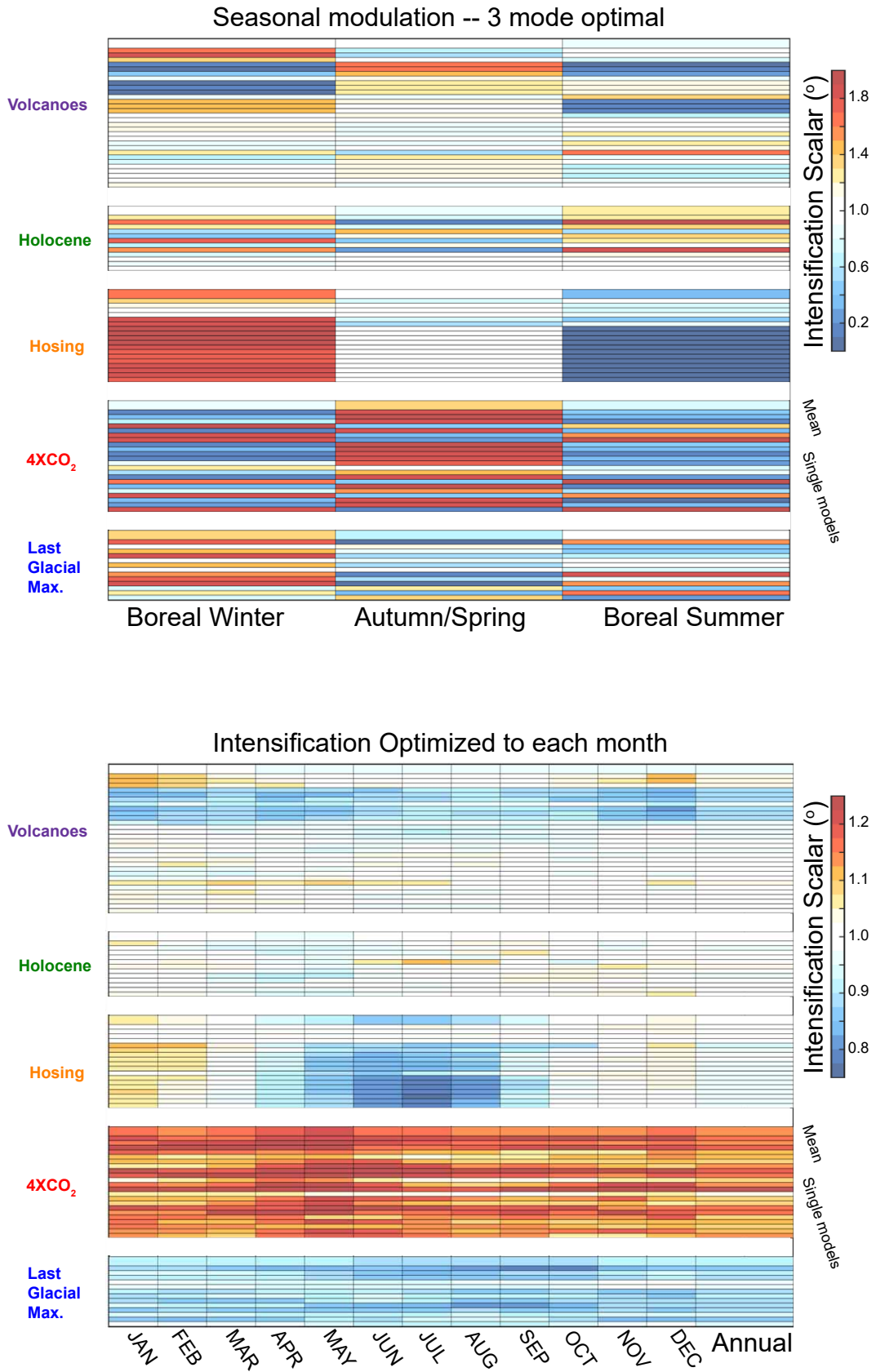
208 **Figure 4.** Analysis of the how the seasonal cycle of changes one tropical precipitation mode manifests in  
 209 the annual mean change of a different mode. (A) The seasonal anomaly of the optimal intensification sorted  
 210 by the annual precipitation centroid ( $P_{CENT}$ ). Models with the the most southward annual  $P_{CENT}$  shift are  
 211 on the bottom of the plot and models with the most northward annual shift are on the top. (B) The seasonal  
 212 anomaly of the optimal shift sorted by the annual mean contraction. Models with the largest annual mean





224 **Figure 6.** Percentage of annual  $\Delta$ P explained by (A) optimal shift/contraction/intensification and (B)

225 modulation of seasonal intensities using 3 modes (Boreal/Austral/Equinox).



226 **Figure 7.** (A) Weighting factors for the 3-mode seasonal modulation clustered by forcing type. The to-  
 -15-  
 227 tal P is = to .25\*Boreal Winter + 0.25\*Boreal Summer + 0.5 Spring/Fall such that the unperturbed annual  
 228 mean would have a value of 1,1,1. (B) The intensification scalar optimized to fit the monthly precipitation for

241 precipitation shift is approximately half of that in the precipitation centroid (regression  
242 coefficient of 0.45) and the optimal shift of the 2D precipitation is even smaller (regres-  
243 sion coefficient = 0.16 – Figure ??B). These results suggest that the metric of the zonal  
244 mean precipitation centroid may overemphasize the magnitude of ITCZ shifts in compre-  
245 hensive modes where zonal inhomogeneities and seasonal variations in the tropical precip-  
246 itation complicate the meaning of a zonal mean ITCZ. More importantly these results and  
247 those presented below question whether the concept of an ITCZ shift is useful for think-  
248 ing about precipitation changes; while the location of the ITCZ in zonally symmetric (i.e  
249 aquaplanet) annual mean simulations where the precipitation is singly peaked at a given  
250 latitude is un-ambiguous, defining the same ITCZ in a system with zonally and seasonally  
251 varying precipitation is very ambiguous with different metrics of the ITCZ location giving  
252 both quantitatively and even qualitatively different results in terms of the direction of the  
253 ITCZ shift results (note the points on quadrants II and IV in Figure ??). Here, we are not  
254 concerned of what metric is the best for the ITCZ location but rather, whether defining an  
255 ITCZ shift by any metric is useful for thinking about precipitation changes in the complex  
256 system or whether such an exercise is simply trying to fit a square peg in a circular hole.

257 The optimal shifting mode explains 9% of the zonal mean precipitation changes in  
258 the ensemble of all experiments considered here and only 1% of the local changes in the  
259 tropical precipitation (Table 1). In the majority of models, the shifting mode explains less  
260 than 2% of the precipitation change even in the zonal mean (Figure ??) . In a minority of  
261 models, the shifting mode explains a much larger fraction (up to 45%) of the zonal mean  
262 precipitation changes explains (note the long tail in red histogram in Figure ??A). The  
263 shifting mode is better than average at explaining the zonal mean precipitation change in  
264 the hosing simulations (highlighted by dark red bars in Figure ??A – ensemble average of  
265 13.2%) and in the mid-Holocene simulations (average of 12.2% and including the two out-  
266 liers on the far right of the distribution). It's unclear whether the increased utility of the  
267 shifting mode in the minority of models is due to differences in the mean state precipita-  
268 tion in the models (i.e. zonal and seasonal homogeneity) or the response to the forcing.

269 Here we emphasize that, in the majority of models, the shifting mode does rather poorly  
 270 at explaining precipitation changes in both the zonal mean and especially in the 2D struc-  
 271 ture.

### 272 **3.2 Contraction mode**

273 The tropical precipitation contracts robustly (significantly different than unity) in  
 274 the ensemble average zonal mean response to  $4XCO_2$  (average contraction scalar =  $0.91 \pm$   
 275  $0.03$ ) and expands with marginal statistical significance ( $1.03 \pm 0.04$ ) in response to LGM  
 276 boundary conditions. The optimal 2D contraction in the LGM and  $4XCO_2$  shows the same  
 277 directionality with reduced amplitude and statistical significance (Table 1). In all other  
 278 experiments, the contraction/expansion differs between ensemble members with no robust  
 279 ensemble average directionality.

280 The contraction of the tropical precipitation found by the optimal fit to the altered  
 281 precipitation under  $4XCO_2$  appears at odds with the tropical expansion found concurrent  
 282 with global warming in observations over the recent decades [Johanson and Fu, 2009]  
 283 and in the modeled response to historical forcing [Lu et al., 2007]. We further analyze  
 284 the changes in the width of the tropical precipitation under  $4XCO_2$  using the following  
 285 methodology:

- 286 1. **A).** The central latitude of the tropical precipitation (i.e. ITCZ location) is defined  
 287 as the latitude that delineates an equal area-average precipitation between  $20^\circ N$   
 288 and  $20^\circ S$  – hereafter referred as the tropical precipitation centroid ( $P_{CENT}$  – most  
 289 equatorward solid vertical lines in Figure ??)
- 290 2. **B).** The central latitude of the tropical precipitation on either side of  $P_{CENT}$  is de-  
 291 fined as the latitude that delineates an equal area-average precipitation between  
 292  $P_{CENT}$  and  $15^\circ$  poleward of  $P_{CENT}$  (the dashed vertical lines in Figure ??). Her-  
 293 after we define this metric as the northern and souther precipitation  $P_{CENT}$ . This  
 294 metric measures how far off the ITCZ the precipitation extends meridionally; be-

295 cause the zonal mean precipitation distribution is bi-modal in most climate mod-  
296 els, this metric roughly coincides with the location of the maximum precipitation  
297 in each of the modes but also takes into account if the precipitation distribution is  
298 asymmetric about the peak as well.

299 3. C). The width of the tropical precipitation is defined as the distance between the  
300 northern and southern precipitaion centroids.

301 In the 4XCO<sub>2</sub> ensemble average, the precipitation increases equatorward of the two  
302 precipitation peaks and is nearly unchanged on the poleward sides of the precipitation  
303 maxima with a concurrent modest equatorward shift in both precipitation maxima (up-  
304 per left panel of Figure ??). As a result, the width of the tropical precipitation contracts  
305 from an average of 14.2° in the PI simulations to 13.4° in the 4XCO<sub>2</sub> simulations. In  
306 fact, the width of tropical precipitation decreases in every one of the 16 4XCO<sub>2</sub> ensemble  
307 members.

308 The contraction mode explains 20.2% of the zonal mean 2.4% of the local structure  
309 of precipitation changes over the ensemble of simulations. The contraction mode exceeds  
310 the utility of the shifting mode by more than a factor of 2 (9.0% and 1.0% respectively  
311 – Table 1). The contraction mode is most useful for describing zonal mean precipitation  
312 changes under 4XCO<sub>2</sub> (33.0%) where there was a robust ensemble average precipitation  
313 contraction and in the Holocene (17.7%) where the ensemble members differ substantially  
314 on the contraction/expansion of the tropical precipitation with no consensus. With the ex-  
315 ception of the hosing experiments, the contraction mode is more useful for describing pre-  
316 cipitation changes than the shifting mode.

### 317 **3.3 Intensification mode**

318 The optimal fit to the perturbed precipitation features robust tropical precipitation  
319 intensification in response to 4XCO<sub>2</sub> (the intensification scalar averages of 1.11 and 1.07  
320 for zonal mean and local cases respectively) and precipitation reduction during the LGM

321 (0.91 and 0.91) as would be expected from the changes in global mean temperature. There  
322 is modest precipitation reduction in the ensemble of hosing experiments (0.97 and 0.95)  
323 and no significant changes in the intensification mode in the Holocene simulations ( $1.00 \pm 0.01$   
324 and  $0.98 \pm 0.01$  – Table 1).

325 The intensification mode explains 35% of the zonal mean and 5.4% of the zonal  
326 mean and 2D pattern of precipitation changes in the ensemble of experiments, exceeding  
327 the combined utility of the shifting and contraction modes in both cases. Not surprisingly,  
328 the intensification mode explains the largest fraction of precipitation changes in the LGM  
329 (57.7% in the zonal mean and 10.1% in the 2D case) and 4XCO<sub>2</sub> (56.6% and 7.0%). In  
330 contrast, the zonal mean intensification mode is less useful than both the shifting and con-  
331 traction modes in the ensemble of hosing and mid-Holocene simulations (Table 1) but still  
332 explains the largest fraction of the local precipitation change in those experiments. The  
333 lack of utility of the intensification mode in explaining zonal mean precipitation changes  
334 in the Holocene experiments is explained as follows: the optimal intensification scalar was  
335 found to be unity in several (3) members resulting in 0% of the precipitation changes ex-  
336 plained by the intensification mode. We emphasize that, for the most part, the intensifi-  
337 cation of climatological pattern of precipitation is the most likely explanation of a given  
338 (zonal mean or local) tropical precipitation change, especially when changes in global  
339 mean temperature are present; the intensification mode is far more useful than even the  
340 combined effect of the shifting and contraction modes.

### 341 **Acknowledgments**

342 All CMIP3 and CMIP5 climate model data were downloaded from the Earth System Grid  
343 Federation (ESGF) node hosted by Lawrence Livermore National Laboratory. AD and  
344 ARA were funded by the National Science Foundation Paleo Perspective on Climate Change  
345 (P2C2) Grant number AGS-1702827.

346 **References**

- 347 Berger, A. (1978), Long-term variations of caloric insolation resulting from Earth's orbital  
 348 element, *Quaternary Res.*, *9*, 139–167.
- 349 Braconnot, P., B. Otto-Bliesner, S. Harrison, S. Joussaume, J. Peterschmitt, A. Abe-  
 350 Ouchi, M. Crucifix, E. Driesschaert, T. Fichefet, C. Hewitt, M. Kageyama, A. Kitoh,  
 351 A. Lâiné, M. Loutre, O. Marti, U. Merkel, G. Ramstein, P. Valdes, S. L. Weber, Y. Yu,  
 352 and Y. Zhao (2007), Results of pmip2 coupled simulations of the mid-holocene and last  
 353 glacial maximum - part 1: experiments and large-scale features., *Climates Past Discuss.*,  
 354 pp. 261–277.
- 355 Braconnot, P., S. Harrison, M. Kageyama, P. Bartlein, V. Masson-Delmotte, A. Abe-Ouchi,  
 356 B. Otto-Bliesner, and Y. Zhao (2012), Evaluation of climate models using paleoclimatic  
 357 data, *Nat. Clim. Chang.*, *2*(6), 417–424.
- 358 Donohoe, A., J. Marshall, D. Ferreira, and D. McGee (2013), The relationship between  
 359 itcz location and atmospheric heat transport across the equator: from the seasonal cycle  
 360 to the last glacial maximum, *J. Climate*, *26*(11), 3597–3618.
- 361 Frierson, D. M. W., and Y.-T. Hwang (2012), Extratropical influence on itcz shifts in slab  
 362 ocean simulations of global warming., *J. Climate*, *25*, 720–733.
- 363 Johanson, C., and Q. Fu (2009), Hadley cell widening: model simulations versus observa-  
 364 tions, *J. Climate*, *22*, 2713–2725.
- 365 Lu, J., G. Vecchi., and T. Reichler (2007), Expansion of the hadley cell under global warm-  
 366 ing, *Geophys. Res. Lett.*, *34*(6), doi:10.1029/2006GL028443.
- 367 Peltier, W. (2004), Global glacial isostasy and the surface of the ice-age earth: The ice-5g  
 368 (vm2) model and grace, *Annu. Rev. Earth Planet. Sci.*, *22*, 111–149.
- 369 Taylor, K., R. Stouffer, and G. Meehl (2012), An overview of cmip5 and the experiment  
 370 design., *Bull. Amer. Meteor. Soc.*, *93*, 485–498.